

# A Two-Step Shearing Strategy To Disperse Long Carbon Nanotubes from Vertically Aligned Multiwalled Carbon Nanotube Arrays for Transparent Conductive Films

Guang-Hui Xu, Qiang Zhang, Jia-Qi Huang, Meng-Qiang Zhao, Wei-Ping Zhou, and Fei Wei\*

Beijing Key Laboratory of Green Chemical Reaction Engineering and Technology, Department of Chemical Engineering, Tsinghua University, Beijing 100084, China

Received August 2, 2009. Revised Manuscript Received September 28, 2009

A surfactant-free two-step shearing strategy was applied to disperse vertically aligned carbon nanotube (VACNT) arrays into individually dispersed CNTs. First, big blocks of VACNT arrays were sheared into fluffy CNTs. The fluffy CNTs were composed of CNT bundles with a diameter of 1–10  $\mu\text{m}$  and a length of several millimeters. After that, the fluffy CNTs were further sheared in liquid phase to obtain individually dispersed CNTs. As comparison, sonication and grinding were also employed for further dispersion of the fluffy CNTs. The length of CNTs dispersed by shearing method was the longest and up to several hundred micrometers. The CNT dispersions from the three methods can be used to fabricate transparent conductive films (TCFs). The TCFs from CNTs dispersed by shearing method showed the highest conductivity at the same transparency. VACNT arrays with a small diameter ( $\sim 10$  nm) were dispersed by the shearing method as well, from which the TCF with a surface resistance of 2.5  $\text{k}\Omega/\square$  and a transparency of 78.6% (at 500 nm) was obtained. The ratio of dc to optical conductivity ( $\sigma_{\text{dc}}/\sigma_{\text{op}}$ ) of the as-dispersed CNT array was 0.711, which can compare beauty with that of single-walled CNTs and double-walled CNTs grown by the CVD process.

## I. Introduction

Because of their exceptional mechanical, electrical, and thermal properties, carbon nanotubes (CNTs) have become one of the focuses of nanoscience and nanotechnology, finding a wide range of applications in composite reinforcement,<sup>1</sup> transparent conductive films (TCFs),<sup>2</sup> etc. For such applications, the CNTs should be individually dispersed in solution or in the polymer matrix; what is more, a longer and straighter CNT is beneficial for electrical and thermal conductivity reinforcement of composites<sup>3</sup> and for the performance improvement of TCFs.<sup>4</sup>

Until now, agglomerated CNTs, in which CNTs are randomly entangled with each other, can be easily mass produced in fluidized bed.<sup>5</sup> They were widely used as raw materials for dispersion and had found amazing applications.<sup>6,7</sup> However, the severe entanglements among CNTs made the procedure for dispersion complex and tedious. Recently, vertically aligned CNT (VACNT) arrays, in which the CNTs with high aspect ratio are well oriented, drew more and more attention. The extraordinary performance was demonstrated and fascinating applications are under development.<sup>8</sup> It has been demonstrated that VACNT arrays can be easily produced by

radial growth on spheres or intercalated growth among a lamellar catalyst.<sup>9,10</sup> 3.0 kg/h of VACNT arrays can intercalated grow among vermiculite with low cost in a fluidized bed reactor.<sup>11</sup> The initial length of CNTs in the array easily reached 1–8 mm. Compared with CNTs in the random agglomerates, the interactions among CNTs in the array are relatively weak, and the length of CNTs increases obviously. The CNTs in the array are with large aspect ratio and have found more and more applications in composites, Li-ion battery, supercapacitor, wave and energy absorbing material, heat transfer device, etc.<sup>10,12–15</sup> The precondition to realize those applications is to obtain CNTs with good dispersion.

Currently, chemical modification of CNTs via covalent bonding and physical modification via noncovalent bonding are adopted for CNT dispersion.<sup>16–18</sup> Aggressive chemical modification at high temperatures created defects on CNTs and shortened the length severely.<sup>19</sup> For physical modification, surfactant micelles, aromatic compounds, and synthetic and biological polymers act as solubilizers to disperse single-walled CNTs via physical adsorption,<sup>18,20,21</sup> which will alter the instinct properties

\*To whom correspondence may be addressed: Tel +86-10-62785464; Fax +86-10-62772051; e-mail wf-dce@tsinghua.edu.cn.

(1) Coleman, J. N.; Khan, U.; Blau, W. J.; Gun'ko, Y. K. *Carbon* **2006**, *44*, 1624.

(2) Wu, Z. C.; Chen, Z. H.; Du, X.; Logan, J. M.; Sippel, J.; Nikolou, M.; Kamaras, K.; Reynolds, J. R.; Tanner, D. B.; Hebard, A. F.; Rinzler, A. G. *Science* **2004**, *305*, 1273.

(3) Deng, F.; Zheng, Q. S. *Appl. Phys. Lett.* **2008**, *92*, 071902.

(4) Simien, D.; Fagan, J. A.; Luo, W.; Douglas, J. F.; Migler, K.; Obrzut, J. *ACS Nano* **2008**, *2*, 1879.

(5) Wei, F.; Zhang, Q.; Qian, W. Z.; Yu, H.; Wang, Y.; Luo, G. H.; Xu, G. H.; Wang, D. Z. *Powder Technol.* **2008**, *183*, 10.

(6) Wang, Q.; Wen, Z. H.; Li, J. H. *Adv. Funct. Mater.* **2006**, *16*, 2141.

(7) Sun, Y.; Bao, H. D.; Guo, Z. X.; Yu, J. *Macromolecules* **2009**, *42*, 459.

(8) Wei, F.; Zhang, Q.; Qian, W. Z.; Xu, G. H.; Xiang, R.; Wen, Q.; Wang, Y.; Luo, G. H. *New Carbon Mater.* **2007**, *22*, 271.

(9) Zhang, Q.; Huang, J. Q.; Zhao, M. Q.; Qian, W. Z.; Wang, Y.; Wei, F. *Carbon* **2008**, *46*, 1152.

(10) Zhang, Q.; Zhao, M. Q.; Liu, Y.; Cao, A. Y.; Qian, W. Z.; Lu, Y. F.; Wei, F. *Adv. Mater.* **2009**, *21*, 2876.

(11) Zhang, Q.; Zhao, M. Q.; Huang, J. Q.; Liu, Y.; Wang, Y.; Qian, W. Z.; Wei, F. *Carbon* **2009**, *47*, 2600.

(12) Moissala, A.; Li, Q.; Kinloch, I. A.; Windle, A. H. *Compos. Sci. Technol.* **2006**, *66*, 1285.

(13) Zhang, H. X.; Feng, C.; Zhai, Y. C.; Jiang, K. L.; Li, Q. Q.; Fan, S. S. *Adv. Mater.* **2009**, *21*, 2299.

(14) Futaba, D. N.; Hata, K.; Yamada, T.; Hiraoka, T.; Hayamizu, Y.; Kakudate, Y.; Tanaike, O.; Hatori, H.; Yumura, M.; Iijima, S. *Nat. Mater.* **2006**, *5*, 987.

(15) Huang, H.; Liu, C. H.; Wu, Y.; Fan, S. S. *Adv. Mater.* **2005**, *17*, 1652.

(16) Nakashima, N.; Fujigaya, T. *Chem. Lett.* **2007**, *36*, 692.

(17) Sun, Y. P.; Fu, K. F.; Lin, Y.; Huang, W. J. *Acc. Chem. Res.* **2002**, *35*, 1096.

(18) Britz, D. A.; Khlbystov, A. N. *Chem. Soc. Rev.* **2006**, *35*, 637.

(19) Liu, J.; Rinzler, A. G.; Dai, H. J.; Hafner, J. H.; Bradley, R. K.; Boul, P. J.; Lu, A.; Iverson, T.; Shelimov, K.; Huffman, C. B.; Rodriguez-Macias, F.; Shon, Y. S.; Lee, T. R.; Colbert, D. T.; Smalley, R. E. *Science* **1998**, *280*, 1253.

(20) Islam, M. F.; Rojas, E.; Bergey, D. M.; Johnson, A. T.; Yodh, A. G. *Nano Lett.* **2003**, *3*, 269.

(21) Wenseleers, W.; Vlasov, I.; Goovaerts, E.; Obratsova, E. D.; Lobach, A. S.; Bouwen, A. *Adv. Funct. Mater.* **2004**, *14*, 1105.

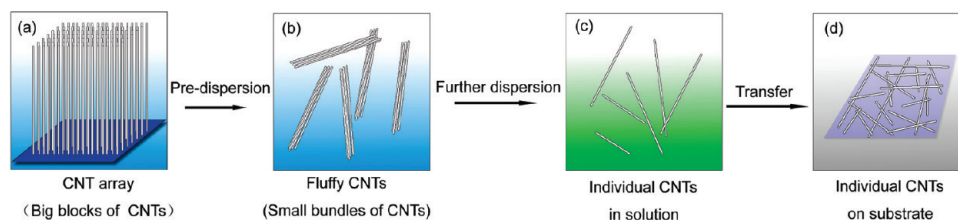


**Figure 1.** Two-step shearing strategy for dispersing CNT arrays into individually dispersed CNTs for TCFs. First, the big blocks of CNT arrays (a) were sheared into fluffy CNTs (b) in the gas phase. The fluffy CNTs were further dispersed into individual CNTs (c) by high-speed shearing in liquid phase. Then individual CNTs were transferred onto a flat substrate (d) for TCFs.

of CNTs and hinder the applications.<sup>22,23</sup> Meanwhile, both chemical and physical modification approaches usually involved the process of sonication, milling, etc.<sup>16–18</sup> After treatment by sonication, the length of CNTs usually decreased sharply to several micrometers.<sup>24</sup> The length of CNTs can even decrease to less than 1  $\mu\text{m}$  if they were treated by milling.<sup>25,26</sup> The maximum length of dispersed CNTs is just 20  $\mu\text{m}$  among many literatures,<sup>24–27</sup> which limited the applications of CNTs in the fields of composites and thermal conductive fluids. It is a critical issue to develop a novel method to increase the length of dispersed CNTs, which includes the use of raw materials with higher aspect ratio and the preservation of the CNT length during the dispersion process.

In this contribution, VACNT array was used as the raw material, and a two-step shearing strategy for dispersing VACNT array was proposed as illustrated in Figure 1. The VACNT arrays were big blocks with highly anisotropic structures (Figure 1a): the CNTs in the array were strong along the *c*-axis direction, but with weak connections among CNTs along the radial direction. A moderate anisotropic shearing force with little damage to the length of CNTs was first applied to large blocks of CNTs to tear them into small fibrous bundles (fluffy CNTs) (Figure 1b). Then the fluffy CNTs were further sheared into individual CNTs (Figure 1c). For the characterization of the length and dispersion state, the CNTs were transferred onto a flat substrate (Figure 1d). The dispersion stability was investigated, and the CNT dispersion was filtrated to fabricate TCFs.

## II. Experimental Section

**Materials.** VACNT arrays fabricated by a floating catalyst chemical vapor deposition (CVD)<sup>9,28</sup> and a thermal CVD method<sup>29</sup> were used, and they were named as VACNT array 1 and VACNT array 2, respectively. The CNTs in VACNT array 1 were with a length of 5.0 mm and a diameter of 30–60 nm, while the CNTs in VACNT array 2 were with a length of 0.2 mm and a diameter of 8–12 nm. Both VACNT arrays were directly used without any specific purification.

**Predispersion of CNTs.** VACNT array 1 was first sheared into fluffy CNTs by high-speed shearing as a pretreatment. About 1.0 g of the VACNT array 1 was placed in a high-speed shearer with a rotor capable of rotating at a speed of 24 000 rpm. After

treatment for 60–600 s, the fluffy CNTs were obtained. Macroscopic photographs were taken using a Nikon 4500 digital camera.

**Further Dispersion of CNTs.** The fluffy CNTs were further dispersed in benzyl alcohol with a concentration of  $\sim 4.0$  mg/L. It was stirred in the disintegrator for 10 min at a rotation speed of 6000–7000 rpm. For comparison, further sonication and grinding were also carried out. The solution was sonicated for 10 h in a sonication bath (frequency of 59 kHz and power of 80 W). For grinding, about 0.1 g of fluffy CNTs was grinded in an agate mortar for about 2.0 h. They are named as shear CNTs, sonication CNTs, and grind CNTs.

For VACNT array 2, shearing was directly applied. A solution with a concentration of  $\sim 0.25$  mg/L was stirred in the disintegrator for 30 min at a rotation speed of 6000–7000 rpm.

**Fabrication of TCFs.** The TCFs were fabricated using the filtration method.<sup>2</sup> The dispersions of both CNT arrays were filtrated through a mixed cellulose ester (MCE) filter membrane (220 nm of pore size). The surface resistance of the film was controlled by filtrating controlled volume of dispersion. The deposited films were then wet transferred onto glass or polyethylene terephthalate (PET) substrates and dried at 75  $^{\circ}\text{C}$  in vacuum overnight under a 27 kPa load. Then the membrane on PET substrate was placed directly in the acetone bath for 20–30 min and then picked up and transferred to a clean acetone bath for another 20–30 min to remove dissolved MCE diffused into the porous film in the first bath. The process was repeated through several baths (usually four times is enough) to ensure the complete removal of MCE. The final bath is typically a methanol bath. The films were picked up and dried to obtain the final CNT film on the PET substrate.

**Characterization.** The VACNT arrays dispersed by different methods were characterized by both scanning electron microscopy (SEM, JSM 7401F) and transmission electron microscopy (TEM, JEM 2010). Some drops from the diluted suspensions were dropped onto a Si wafer or a copper grid and dried in an oven (80  $^{\circ}\text{C}$ ) for the observation for SEM and TEM, respectively. The optical properties of CNT dispersions and TCFs (without PET substrate) were measured by an A-722 grating spectrophotometer at a wavelength of 500 nm. The surface resistance of TCFs was obtained by a four-probe method. Raman experiments were performed with a Raman spectrophotometer Renishaw, RM2000 in ambient conditions. The spectra were recorded using a He–Ne laser excitation line of 633 nm. The raw materials of VACNT array 1 and VACNT array 2 and grind CNTs were directly used in powder form (on glass slides). The dispersions of shear CNTs and sonication CNTs were filtrated through MCE filter membranes, washed with deionized water, and dried at 75  $^{\circ}\text{C}$  in an oven. Then the MCE membrane was dissolved in several acetone baths and a final methanol bath as described above. Opaque thick CNT films were picked up by glass slides and dried to get the sample for Raman analysis.

## III. Results and Discussion

### 3.1. Predispersion of VACNT Array 1 into Fluffy CNTs.

The VACNT array 1 obtained by a 150 min synchronous growth<sup>28</sup> were large blocks with a size of several millimeters

(22) Geng, H. Z.; Kim, K. K.; So, K. P.; Lee, Y. S.; Chang, Y.; Lee, Y. H. *J. Am. Chem. Soc.* **2007**, *129*, 7758.

(23) Bryning, M. B.; Milkie, D. E.; Islam, M. F.; Kikkawa, J. M.; Yodh, A. G. *Appl. Phys. Lett.* **2005**, *87*, 161909.

(24) Hilding, J.; Grulke, E. A.; Zhang, Z. G.; Lockwood, F. J. *Dispersion Sci. Technol.* **2003**, *24*, 1.

(25) Kukovec, A.; Kanyo, T.; Konya, Z.; Kiricsi, I. *Carbon* **2005**, *43*, 994.

(26) Darsono, N.; Yoon, D. H.; Kim, J. Y. *Appl. Surf. Sci.* **2008**, *254*, 3412.

(27) Glory, J.; Mierczynska, A.; Pinault, M.; Mayne-L'Hermite, M.; Reynaud, C. *J. Nanosci. Nanotechnol.* **2007**, *7*, 3458.

(28) Zhang, Q.; Zhou, W. P.; Qian, W. Z.; Xiang, R.; Huang, J. Q.; Wang, D. Z.; Wei, F. *J. Phys. Chem. C* **2007**, *111*, 14638.

(29) Zhang, X. B.; Jiang, K. L.; Teng, C.; Liu, P.; Zhang, L.; Kong, J.; Zhang, T. H.; Li, Q. Q.; Fan, S. S. *Adv. Mater.* **2006**, *18*, 1505.

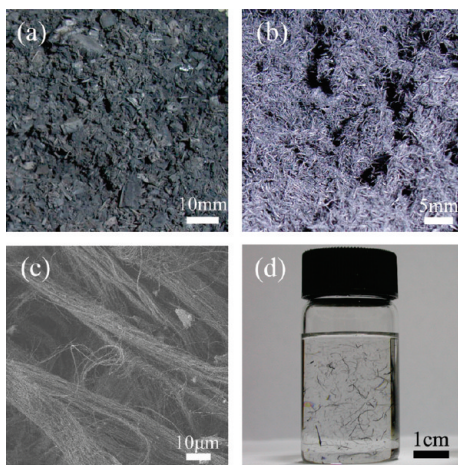


**Figure 2.** Macroscopic images of big blocks of CNT arrays (a), fluffy CNTs obtained after high-speed shearing (b), and fluffy CNTs in benzyl alcohol (d). (c) is the SEM image of fluffy CNTs.

(Figure 2a) and a length of about 5.0 mm. The array was treated by a high speed shearing in air, and macroscopically fluffy CNTs were obtained (Figure 2b), whose apparent density was about 4.0 g/L. From the SEM image, it can be observed that the fluffy CNTs consisted of CNT bundles with bundle diameters of 1–10  $\mu\text{m}$  (Figure 2c). The CNTs in the VACNT array showed an anisotropic connection along the CNT radial direction where weak connections existed. When the arrays were sheared, they were torn into pieces along the  $c$ -axis direction. The pieces became smaller with prolonged shearing duration. As a result, fluffy CNTs were obtained by shearing the VACNT array. The high-speed shearing in air was effective for the predispersion of CNT arrays. However, in fluffy CNTs, the CNT bundles can hardly be further torn into smaller pieces due to the limitation of rotation speed and the thickness of rotor (0.5 mm). The shock might have been relaxed by bundle torsion due to the flexibility of CNT bundle.<sup>30</sup> In the fluffy CNTs, the length of CNT bundles was still at the order of several millimeters (Figure 2d). Taking advantage of the higher shearing force in the liquid phase, the fluffy CNTs were further sheared in the liquid phase to obtain individually dispersed CNT in the second step.

### 3.2. Dispersion of Fluffy CNTs by Different Methods.

Various kinds of solvents, such as ethanol, ethylene glycol, benzyl alcohol, *N*-methyl-2-pyrrolidone (NMP), and dimethylformamide (DMF), were selected for CNT dispersion. After the same procedure, we found individually dispersed CNTs can be easily obtained in benzyl alcohol. This was mainly attributed to the  $\pi$ - $\pi$  stacking between the benzyl ring in benzyl alcohol and CNTs. Furthermore, the viscosity of benzyl alcohol is 5.474 mPa·s, which was obviously higher than that of DMF and NMP (0.796 and 1.666 mPa·s at 25 °C, respectively) and thus was beneficial to form the high shearing force environment. Some other kinds of solvents, such as 1,2-dichlorobenzene and chloroform, might be more appropriate for two-step shearing for CNT dispersion.<sup>31,32</sup> But here, to illustrate the strategy easily, we choose benzyl alcohol as the solvent.

The individual CNTs dispersed in benzyl alcohol were further characterized. Figure 3 shows the SEM images and length

distribution of CNTs treated by different methods (shearing, sonication, and grinding). The CNTs were all simply lapped on each other, and no entanglement was observed (Figure 3a–c). As measured from Figure 3a,b, the length of shear CNTs was 5.1–106.1  $\mu\text{m}$  and sonication CNTs was 7.4–113.9  $\mu\text{m}$ . The length distributions of both shear CNTs and sonication CNTs were between normal and log-normal distribution (Figure 3d,e). The average length and standard deviation for shear CNTs and sonication CNTs were  $38.5 \pm 19.3 \mu\text{m}$  and  $31.4 \pm 20.1 \mu\text{m}$ , respectively. The length of grind CNTs distributed uniformly with an average value and standard deviation of  $1.5 \pm 0.8 \mu\text{m}$  (Figure 3c,f). The length of grind CNTs showed a narrow normal distribution, which is in accordance with previous report of Kukovec et al.<sup>25</sup>

After shearing in a solvent, the dispersion was standing for 30 min and carefully decanted (Figure 4a (I)). Figure 4a (II, III) shows the macroscopic images of CNTs dispersed by sonication and grinding. They all looked transparent and homogeneous. The absorbance vs concentration curves of different CNT dispersions are shown in Figure 4b. The absorbance was proportional to the concentration. The mass absorbance coefficients were 34.53 (I), 39.02 (II), and 49.18 mL  $\text{mg}^{-1} \text{cm}^{-1}$  (III), respectively. The sequence of mass absorbance coefficients in increase order was shear CNTs < sonication CNTs < grind CNTs, which was opposite with the length sequence shown in Figures 3 and 4. As the length of CNTs increased, the mass absorbance coefficient decreased. Very recently, Moon et al. reported that the absorption coefficients were found to be  $\sim 42.58 \text{ mL mg}^{-1} \text{cm}^{-1}$  for long CNTs (length of  $1000 \pm 200 \text{ nm}$ ) and  $\sim 34.88 \text{ mL mg}^{-1} \text{cm}^{-1}$  for short CNTs (length of  $200 \pm 40 \text{ nm}$ ).<sup>33</sup> However, herein the length distributions of CNTs were larger, and the CNTs were dispersed without covalent functionalization. As illustrated in inset images of Figure 4b, the length of CNTs dispersed by shearing and sonication was much larger than the wavelength of visible light. At the same concentration, the longer the CNTs, the larger the gap among CNTs; thus, fewer photons were scattered by CNTs. Therefore, the mass absorbance coefficient can be regarded as an effective macroscopic parameter to evaluate the length of dispersed CNTs in solution.

### 3.3. Mechanism of Shearing To Disperse Fluffy CNTs. It

is noticed that the CNTs were shortened after the liquid phase dispersion. The stress applied on a single CNT during dispersion process was a key point to understand those phenomena. As proved by both theoretical calculation<sup>34</sup> and experimental results,<sup>35</sup> a stress as strong as  $10^9$ – $10^{10}$  Pa can be generated during a simple grinding process. Also, the pestle contact with the CNTs in a noncushioned way, plus the brittleness caused by large diameter, led to the fracture of long CNTs into tiny pieces. As shown in Figure S1a,b of the Supporting Information, the fracture of the grind CNTs was irregular and the graphite layer was exfoliated and collapsed severely. Meanwhile, the wall of CNTs was distorted seriously, which were in agreement with the results in the literature.<sup>26</sup> The Raman spectrum is an important way to characterize the defect densities of carbon products macroscopically. Here, the ratio of intensity of D peak to G peak ( $I_D/I_G$ ) can be used to characterize the degree of defect of multiwalled CNTs (MWCNTs). The  $I_D/I_G$  ratio of VACNT array 1 was 0.647, while the  $I_D/I_G$  ratio of grind CNTs increased to 0.911 (Figure S2).

(30) Zhang, Q.; Xu, G. H.; Huang, J. Q.; Zhou, W. P.; Zhao, M. Q.; Wang, Y.; Qian, W. Z.; Wei, F. *Carbon* **2009**, *47*, 538.

(31) Bahr, J. L.; Mickelson, E. T.; Bronikowski, M. J.; Smalley, R. E.; Tour, J. M. *Chem. Commun.* **2001**, 193.

(32) Bergin, S. D.; Nicolosi, V.; Streich, P. V.; Giordani, S.; Sun, Z. Y.; Windle, A. H.; Ryan, P.; Niraj, N. P. P.; Wang, Z. T. T.; Carpenter, L.; Blau, W. J.; Boland, J. J.; Hamilton, J. P.; Coleman, J. N. *Adv. Mater.* **2008**, *20*, 1876.

(33) Moon, Y. K.; Lee, J.; Lee, J. K.; Kim, T. K.; Kim, S. H. *Langmuir* **2009**, *25*, 1739.

(34) Urakaev, F. K.; Boldyrev, V. V. *Powder Technol.* **2000**, *107*, 93.

(35) Burns, J. H.; Bredig, M. A. *J. Chem. Phys.* **1956**, *25*, 1281.

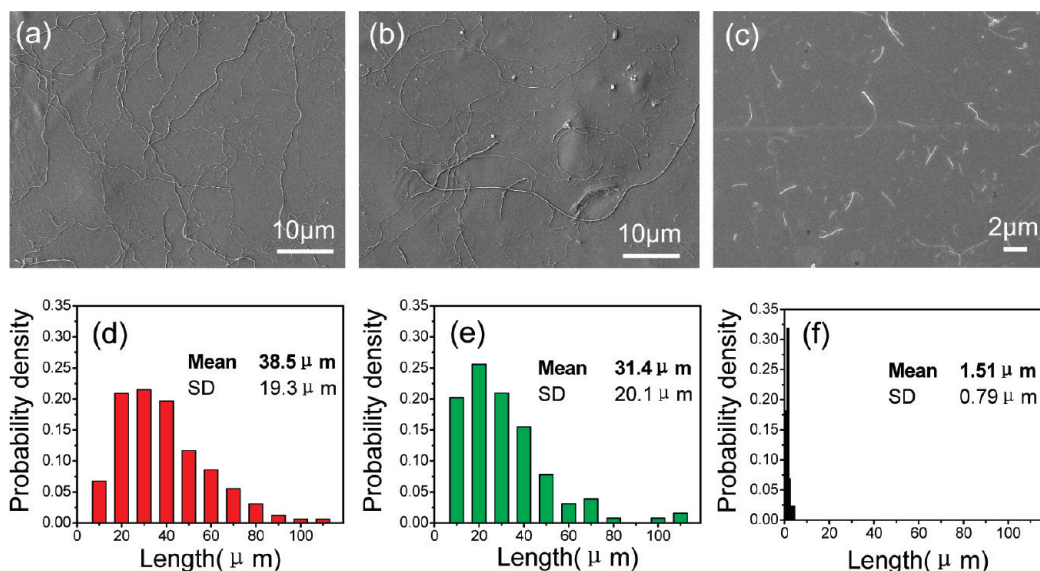


**Figure 3.** (a–c) and (d–f) are SEM images and length distribution of CNTs dispersed by shearing, sonication, and grinding, respectively.

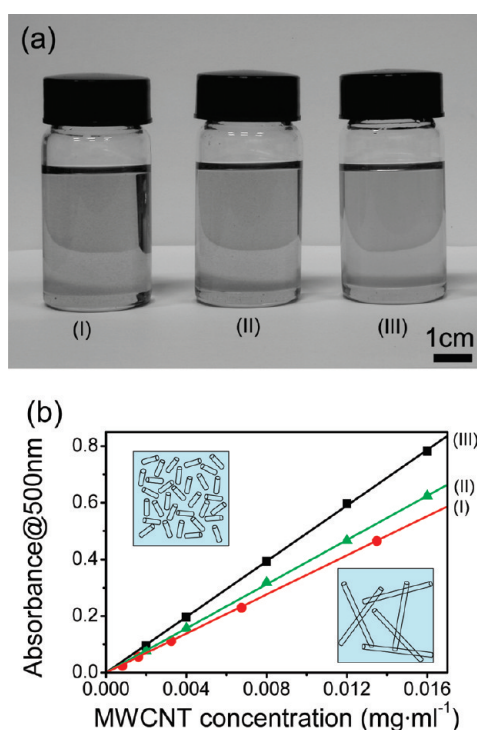


**Figure 4.** (a, b) Macroscopic images and the absorbance vs concentration curves of CNTs dispersed by different methods: (I) shearing (●), (II) sonication (▲), and (III) grinding (■).

For sonication, the ultrasonic waves of high-intensity ultrasound generate cavitations in liquids. The cavitations result in extreme shearing stress locally. As estimated by Ahir et al.,<sup>36</sup> the maximum tensile stress generated by viscous forces near the imploding bubble was as high as  $\sigma_t \sim 70$  GPa, which was strong enough to break most of the nanotubes.<sup>37,38</sup> However, sonication is usually carried out in the liquid phase due to the cushion of solvent; the viscous force decays as the length decreases and finally reaches a

threshold that will no longer break the tube. Thus, the length of CNT will reach a critical value and has been demonstrated in Hilding's experiment.<sup>24</sup> After sonication (Figure S1c,d), the fracture was irregular and the graphite layers were destroyed. Some of them were dilacerated, and also the graphite walls were with some distortion. Such observation is in accordance with that reported by Lu et al.<sup>39</sup> The  $I_D/I_G$  ratio of sonication CNTs was slightly increased from 0.647 to 0.656 (Figure S2).

Here, we used the classical solution to calculate the minimum shearing stress needed to fully disperse the long carbon nanotubes (see the Supporting Information). For two identical tubes with the diameter  $d = 30$  nm and contour length  $L = 5$  mm, aligned parallel to each other with a separation  $H = 30$  nm, the average shear strength should be over  $\sim 160$  Pa to disperse the CNTs. In our experiment, the average shear stress calculated was about 5 Pa. However, the flow in the disintegrator is not simple shear flow and eddy current exist in some local space. Then the shearing stress easily exceeded 160 Pa, which was adequate to separate CNTs apart. This stress is not strong enough to break the perfect structure of CNTs. But CNTs tended to be fractured at the position of defects formed during the CVD process. The fracture of shear CNT was relatively regular and the graphite layers were almost broken at the same position, and the tube wall was still straight with little distortion (Figure S1e,f). The  $I_D/I_G$  ratio of shear CNTs even decreased from 0.647 to 0.618 (Figure S2), which can be attributed to the removal of amorphous carbon during the dispersion process. It can be seen that both the TEM and high-resolution TEM observations (Figure S1) agreed well with the Raman spectra results (Figure S2). The sequence of the degree of defects was shear CNTs < sonication CNTs < grind CNTs.

**3.4. Stability of CNT Dispersion.** The dispersion stability of CNT dispersion is a very important aspect. Here, we investigated the optical properties of CNT dispersion to characterize the stability.<sup>40</sup> Because of the high aspect ratio, the CNTs tend to flocculate and aggregate to form loose floccules moving randomly.<sup>41</sup> Then the read of transmittance will have a wide flounce

(36) Ahir, S. V.; Huang, Y. Y.; Terentjev, E. M. *Polymer* **2008**, *49*, 3841.

(37) Yu, M. F.; Lourie, O.; Dyer, M. J.; Moloni, K.; Kelly, T. F.; Ruoff, R. S. *Science* **2000**, *287*, 637.

(38) Peng, B.; Locascio, M.; Zapol, P.; Li, S. Y.; Mielke, S. L.; Schatz, G. C.; Espinosa, H. D. *Nat. Nanotechnol.* **2008**, *3*, 626.

(39) Lu, K. L.; Lago, R. M.; Chen, Y. K.; Green, M. L. H.; Harris, P. J. F.; Tsang, S. C. *Carbon* **1996**, *34*, 814.

(40) Lisunova, M. O.; Lebovka, N. I.; Melezhyk, E. V.; Boiko, Y. P. *J. Colloid Interface Sci.* **2006**, *299*, 740.

(41) Li, Z. F.; Luo, G. H.; Zhou, W. P.; Wei, F.; Xiang, R.; Liu, Y. P. *Nanotechnology* **2006**, *17*, 3692.

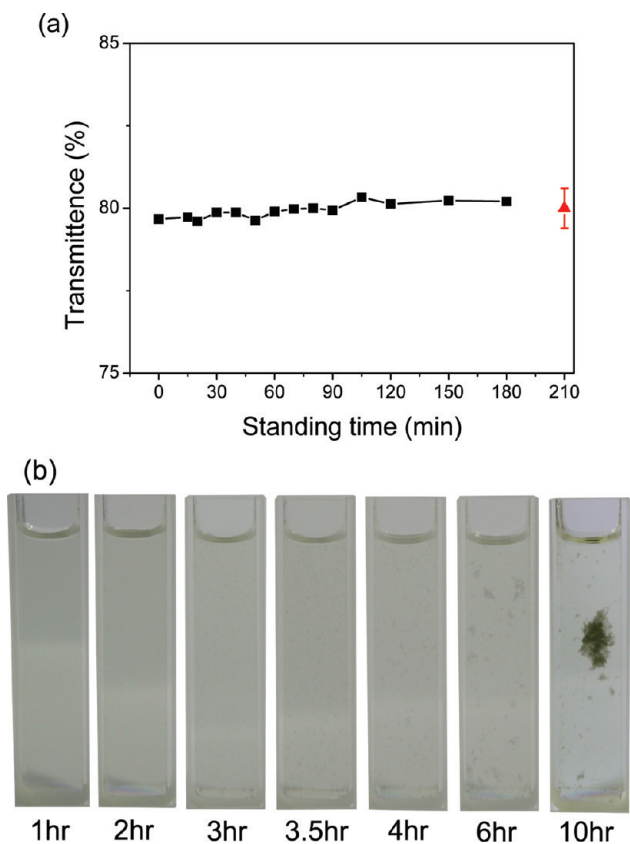


**Figure 5.** Transmittance vs standing time curve (a) and the macroscopic images of CNT dispersed by the shearing method after different standing time.

range, and this phenomenon can be used as the criteria of transition from stable to unstable. The transmittance of CNT dispersion is stable in 180 min and showed wide flounce at 210 min (Figure 5a). This is in good accordance with the macroscopic images (Figure 5b). When the time increased to 3.5 h, small agglomerates appeared and grew up into floccules with a size of several millimeters. Finally, large agglomerate formed and suspended in the solution. The CNTs was prone to lap on each other due to large aspect ratio, and loose ellipsoidal agglomerate formed, accordingly. However, when shaking the solution, the floccules disappeared and the solution became uniform again. So these floccules were thought to be “soft agglomerates” which can be redispersed easily. The stability can be improved by functionalization or the assistance of surfactants. However, it will generate negative effects for further applications in the fields of electrical and thermal conductivity enhancement.<sup>22,23</sup>

**3.5. TCFs Made from VACNT Array 1 Dispersed by Different Methods.** The shear CNTs possessed a large aspect ratio, which benefited the applications in the fields of composites, thermal conductive fluids, and TCFs, etc.<sup>3,4,42</sup> Research works<sup>22,43–48</sup> have

(42) Glory, J.; Bonetti, M.; Helezen, M.; Mayne-L’Hermite, M.; Reynaud, C. *J. Appl. Phys.* **2008**, *103*, 7.

(43) Zhang, D. H.; Ryu, K.; Liu, X. L.; Polikarpov, E.; Ly, J.; Tompson, M. E.; Zhou, C. W. *Nano Lett.* **2006**, *6*, 1880.

(44) Wang, Y.; Di, C. A.; Liu, Y. Q.; Kajihara, H.; Ye, S. H.; Cao, L. C.; Wei, D. C.; Zhang, H. L.; Li, Y. M.; Noda, K. *Adv. Mater.* **2008**, *20*, 4442.

(45) Pei, S. F.; Du, J. H.; Zeng, Y.; Liu, C.; Cheng, H. M. *Nanotechnology* **2009**, *20*, 235707.

(46) Green, A. A.; Hersam, M. C. *Nano Lett.* **2008**, *8*, 1417.

(47) Wei, J. Q.; Jia, Y.; Shu, Q. K.; Gu, Z. Y.; Wang, K. L.; Zhuang, D. M.; Zhang, G.; Wang, Z. C.; Luo, J. B.; Cao, A. Y.; Wu, D. H. *Nano Lett.* **2007**, *7*, 2317.

(48) Xiao, L.; Chen, Z.; Feng, C.; Liu, L.; Bai, Z. Q.; Wang, Y.; Qian, L.; Zhang, Y. Y.; Li, Q. Q.; Jiang, K. L.; Fan, S. S. *Nano Lett.* **2008**, *8*, 4539.

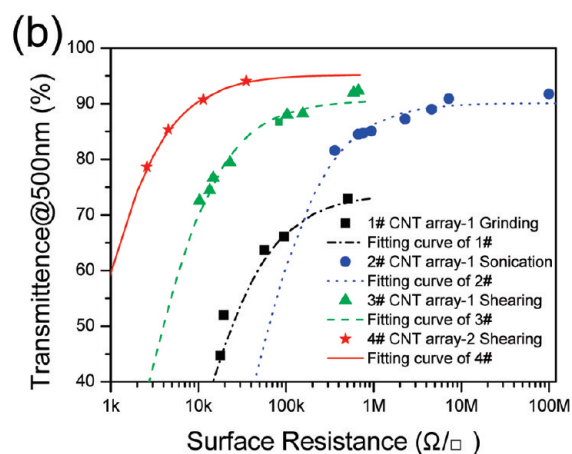
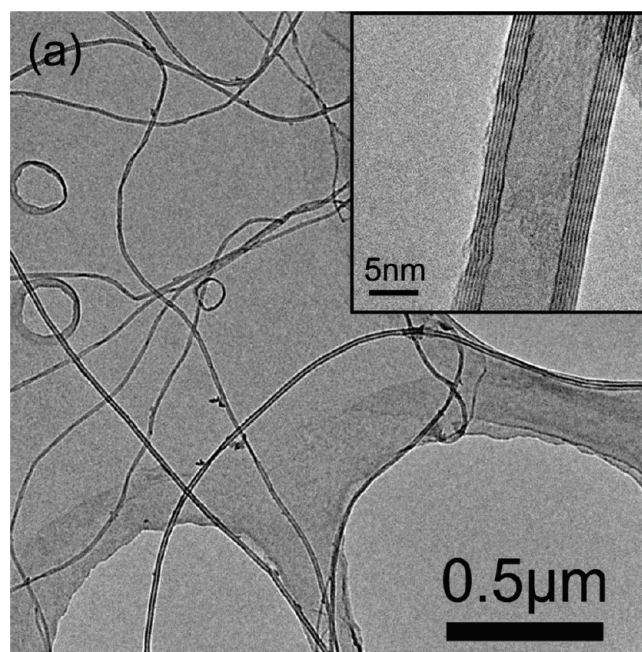


**Figure 6.** (a) VACNT array 2 with diameter of  $\sim 10$  nm dispersed by shearing method. The inset image shows the HRTEM image of one tube. (b) Surface resistance vs transmittance of transparent conductive films using VACNT array 1 dispersed by shearing ( $\blacktriangle$ ), sonication ( $\bullet$ ), and grinding ( $\blacksquare$ ) and using VACNT array 2 dispersed by shearing ( $\star$ ).

shown that CNT TCFs possess high optical transparency and electrical conductivity, which now has matched the demand for some applications such as touch screens ( $500 \Omega/\square$  at 85% T is needed for practical applications). Moreover, CNT TCFs are far more flexible and environmentally resistant than ITO film,<sup>49</sup> in addition to that carbon is a much more abundant resource than indium. Consequently, CNT TCFs are considered to be one of the most promising fields for the near-term industrial application of CNTs. Most researchers use surfactant to disperse single-walled CNTs (SWCNTs) for the fabrication of TCFs.<sup>2,22,43–45</sup> The existence of insulating surfactant caused larger contact resistance between tubes, and the surfactant has to be removed by immersing in nitric acid, etc.<sup>22</sup> Herein the CNTs dispersed by the three methods were used to prepare TCFs. As shown in Figure 6b, the performances were  $10.3 \text{ k}\Omega/\square$  at 72.5% T,  $360 \text{ k}\Omega/\square$  at 81.6% T, and  $507 \text{ k}\Omega/\square$  at 72.9% T for TCFs made from shear CNTs,

(49) Saran, N.; Parikh, K.; Suh, D. S.; Munoz, E.; Kolla, H.; Manohar, S. K. *J. Am. Chem. Soc.* **2004**, *126*, 4462.

**Table 1. Fitting Parameters of CNT TCFs in the Literature and This Work**

type of CNTs	preparation	diameter (nm)	treatment	$t$	$\sigma_{dc}/\sigma_{op}$	$\sigma_{dc}$ (S/cm)	$\sigma_{op}$ (S/cm)	refs
SWCNTs	HiPCO	2	chloroform	1	~1			53
SWCNTs	arc carbon solutions		SDS	1	9.143	1600	175	54
SWCNTs	CO/Co–Mo	0.6–0.9	DMF	1	0.256			52
SWCNTs	laser	1.2–1.7			1.667			
DWCNTs	Fe–Mo/MgO	1.5–2.9			0.588			
RF-MWCNTs	Fe–Co/CaCO <sub>3</sub>	5–35			0.357			
SWCNTs	arc Ijin	1.3–1.5	SDS	1	13.0	2300	177	56
			SDBS		10.5	1900	180	
SWCNTs	arc Ijin	1.3–1.5	SWCNTs/PEDOT:PSS	1	15.0	1650	110	57
	HiPCO	~1			3.3	400	110	
SWCNTs	arc Ijin	1.3–1.5	SDS	0.999	7.525			55
DWCNTs	arc Ijin	2–3		0.992	0.864			
t-MWCNTs	CCVD	4–6		0.962	0.248			
MWCNTs	CCVD	10–16		0.884	0.161			
SWCNTs	arc Ijin	1.3–1.5	SDS	1	10.1	1500	150	58
			HNO <sub>3</sub>		25.3	5700	225	
MWCNTs	floating catalyst CVD	30–60	grinding	0.738	0.036			this work
			sonication	0.901	0.009			
	thermal CVD	8–12	shearing	0.907	0.136			
			shearing	0.952	0.711	~100	~140	

sonication CNTs, and grind CNTs. The sequence of surface resistance at the same transmittance was shear CNTs < sonication CNTs < grind CNTs. These results consisted well with the length order in Figure 3 and the TCFs from SWCNTs with different length.<sup>4</sup>

**3.6. Dispersion of VACNT Array 2 and Performance of TCFs.** The two-step shearing method is a general effective strategy for dispersing CNT arrays. To prove this point, VACNT array 2 with a diameter of about 10 nm was also dispersed by this shearing method. As shown in Figure 6a, in the visual field, the CNTs were all individually dispersed, indicating the generality of this shearing method in the dispersion of CNTs with different diameters. Both VACNT array 1 and VACNT array 2 dispersed by shearing method showed clean walls without surfactant contamination (see the inset images of Figure 6a and Figure S1e). VACNT array 2 dispersed by the shearing method was also used to fabricate TCFs. At the same transmittance, the surface resistance was decreased by one order compared with that fabricated by VACNT array 1, as shown in Figure 6b. Thus, the CNTs with smaller diameter and fewer wall numbers were beneficial for applications as TCFs, which is in accordance with the literature.<sup>50–52</sup> In our case, the TCFs from VACNT array 2 were with a resistance of about 2.5 k $\Omega$ /□ at a transmittance of 78.6% (500 nm). As indicated from the visible spectra, an even higher transmittance of 79.7% at a wavelength of 550 nm (commonly used in literatures) was observed (Figure S3).

To describe the performance of the TCFs more clearly, the electro-optical properties for a metallic thin film (film thickness much smaller than wavelength of light) in air was used, which was similar to many reports for SWCNT TCFs.<sup>53,54</sup> It can be expressed as follows:

$$T = \left(1 + \frac{Z_0 \sigma_{op}}{2R_s \sigma_{dc}}\right)^{-2} \quad (1)$$

where  $\sigma_{dc}$  is the dc conductivity,  $\sigma_{op}$  is the optical conductivity, and  $Z_0$  is the characteristic impedance of free space (~376.73  $\Omega$ ).

A material with relatively high conductivity and yet low optical absorbance as manifested by a large ratio of dc to optical conductivity,  $\sigma_{dc}/\sigma_{op}$ , is strongly demanded for thin, transparent, conductive films for electrode applications in devices from liquid crystal displays to organic light-emitting diodes and solar cells. Here, the thickness is about 50–100 nm for MWCNT film, which cannot meet the assumption that the film thickness was much smaller than wavelength of light (500 nm). Thus, the modified equation by Geng et al.<sup>55</sup> as follows was used:

$$T = t \left(1 + \frac{Z_0 \sigma_{op}}{2R_s \sigma_{dc}}\right)^{-2} \quad (2)$$

where  $t$  presents the diameter effect of MWCNT film. The fitting curves are shown in Figure 6b which fitted well with the experimental data. The fitting results and other reported data are presented in Table 1.<sup>52–58</sup> It can be found that  $t$  is lower with the increase of film thickness. For VACNT array 1, the diameter is large and both  $t$  and  $\sigma_{dc}/\sigma_{op}$  are small. The  $\sigma_{dc}/\sigma_{op}$  of the shear CNTs, sonication CNTs, and grind CNTs were just 0.136, 0.009, and 0.036, respectively. For VACNT array 2, the diameter of CNTs was small (8–12 nm), and the  $\sigma_{dc}/\sigma_{op}$  value of VACNT array 2 dispersed by shearing method was 0.711. Geng et al. reported that TCFs obtained from sodium dodecyl sulfonate (SDS)-assisted dispersed MWCNTs were with a  $\sigma_{dc}/\sigma_{op}$  value of 0.161.<sup>55</sup> Li reported that TCFs obtained from MWCNTs dispersed in DMF by sonication were with a  $\sigma_{dc}/\sigma_{op}$  value of 0.357.<sup>52</sup> The reported  $\sigma_{dc}/\sigma_{op}$  values of double-walled CNTs (DWCNT) TCFs were about 0.588–0.864.<sup>52,55</sup> Some  $\sigma_{dc}/\sigma_{op}$  values of SWCNT TCFs were less than 0.7.<sup>52</sup> SWCNTs obtained from arc discharge are always with a quite high  $\sigma_{dc}/\sigma_{op}$  value over 10.<sup>56–58</sup> These indicated that the VACNT array 2 dispersed by the shearing method were with long length and good dispersion, which can compare beauty with SWCNTs and DWCNTs grown by CVD. The dc conductivity of TCFs from VACNT array 2 was

(55) Geng, H. Z.; Lee, D. S.; Kim, K. K.; Kim, S. J.; Bae, J. J.; Lee, Y. H. *J. Korean Phys. Soc.* **2008**, *979*.

(56) Doherty, E. M.; De, S.; Lyons, P. E.; Shmeliov, A.; Nirmalraj, P. N.; Scardaci, V.; Joimel, J.; Blau, W. J.; Boland, J. J.; Coleman, J. N. *Carbon* **2009**, *47*, 2466.

(57) De, S.; Lyons, P. E.; Sorel, S.; Doherty, E. M.; King, P. J.; Blau, W. J.; Nirmalraj, P. N.; Boland, J. J.; Scardaci, V.; Joimel, J.; Coleman, J. N. *ACS Nano* **2009**, *3*, 714.

(58) Geng, H. Z.; Lee, D. S.; Kim, K. K.; Han, G. H.; Park, H. K.; Lee, Y. H. *Chem. Phys. Lett.* **2008**, *455*, 275.

(50) Geng, H. Z.; Kim, K. K.; Lee, K.; Kim, G. Y.; Choi, H. K.; Lee, D. S.; An, K. H.; Lee, Y. H.; Chang, Y.; Lee, Y. S.; Kim, B.; Lee, Y. J. *Nano* **2007**, *2*, 157.

(51) Moon, J. S.; Park, J. H.; Lee, T. Y.; Kim, Y. W.; Yoo, J. B.; Park, C. Y.; Kim, J. M.; Jin, K. W. *Diamond Relat. Mater.* **2005**, *1882*.

(52) Li, Z. R.; Kandel, H. R.; Dervishi, E.; Saini, V.; Xu, Y.; Biris, A. R.; Lupu, D.; Salamo, G. J.; Biris, A. S. *Langmuir* **2008**, *24*, 2655.

(53) Hu, L.; Hecht, D. S.; Gruner, G. *Nano Lett.* **2004**, *4*, 2513.

(54) Zhou, Y. X.; Hu, L. B.; Gruner, G. *Appl. Phys. Lett.* **2006**, *88*, 123109.

$\sim 100$  S/cm, which was lower than that of SWCNT TCFs.<sup>54,56,58</sup> Using the dc conductivity, the optical conductivity of TCFs from VACNT array 2 was  $\sim 140$  S/cm at 500 nm, which was comparable to results in the literature<sup>54,56,58</sup> and  $\sigma_{\text{op}} = 200$  S/cm obtained from buckypaper.<sup>59</sup>

The performance of the as-obtained MWCNT film has fulfilled the requirements for various applications such as electrostatic dissipation and electromagnetic shielding inside of cathode ray tubes.<sup>60</sup> Taking advantages of the low-cost mass production of VACNT arrays and the simple dispersion strategy, it is promising for the real application of long CNTs in the field of TCFs. Furthermore, the long individual CNTs in benzyl alcohol can also be used to fabricate strong CNT films, sensors, and other devices in the future.

#### IV. Conclusions

In conclusion, by a two-step shearing strategy, we have obtained individually dispersed CNTs from VACNT arrays. First, big blocks of VACNT arrays were sheared into fluffy CNTs. The fluffy CNTs were composed of CNT bundles with a diameter of 1–10  $\mu\text{m}$  and a length of several millimeters. After that, fluffy CNTs were further sheared in liquid phase to obtain individually dispersed CNTs. As a comparison, sonication and grinding were also employed for further dispersion of the fluffy CNTs. The length of CNTs dispersed by the shearing method was the longest and with an average length of about 40  $\mu\text{m}$ . The length can be further validated by measuring the optical properties of CNT dispersions. Avoiding the local strong shear stress generated

in sonication or grinding, the shearing treatment along the axis direction is effective and gentler to preserve the CNT length. The dispersion possesses good stability and is stable within 3.5 h. The CNTs dispersed by the shearing method can be used to fabricate TCFs and showed a better performance (10.3  $\text{k}\Omega/\square$  at 72.5% T) over that from sonication CNTs and grind CNTs. The shearing method was effective for the dispersion of VACNT arrays with a small diameter ( $\sim 10$  nm) as well. The performance of TCFs was further improved, and the surface resistance was about 2.5  $\text{k}\Omega/\square$  with a transparency of 78.6% (at 500 nm). The  $\sigma_{\text{dc}}/\sigma_{\text{op}}$  value of VACNT array 2 dispersed by the shearing method was 0.711, which can compare beauty with SWCNTs and DWCNTs grown by the CVD process. The reported two-step dispersion strategy provides a general method to obtain individual CNTs with the length of tens of micrometers for further applications in composites and devices.

**Acknowledgment.** We acknowledge Ying-Hao Zhang for the figure preparation and the financial support by the Foundation for the Natural Scientific Foundation of China (No. 20736007, No. 2007AA03Z346) and the China National Program (No. 2006CB932702).

**Supporting Information Available:** Calculation of shear stress needed to disperse long CNTs; TEM and HRTEM images of CNTs dispersed by shearing, sonication, and grinding (Figure S1); Raman spectra of the raw materials of VACNT array 1, shear CNTs, sonication CNTs, and grind CNTs (Figure S2); visible spectra of transparent conductive films made from VACNT array 2 dispersed by shearing method (Figure S3). This material is available free of charge via the Internet at <http://pubs.acs.org>.

(59) Ugawa, A.; Hwang, J.; Gommans, H. H.; Tashiro, H.; Rinzler, A. G.; Tanner, D. B. *Curr. Appl. Phys.* **2001**, *1*, 45.

(60) Kaempgen, M.; Duesberg, G. S.; Roth, S. *Appl. Surf. Sci.* **2005**, *252*, 425.